International Journal of Applied Earth Observation and Geoinformation 11 (2009) 244–255

Contents lists available at ScienceDirect

International Journal of Applied Earth Observation and Geoinformation

journal homepage: www.elsevier.com/locate/jag

Remote sensing of spider mite damage in California peach orchards

Eike Luedeling [a], Adam Hale [a], Minghua Zhang [a,*], Walter J. Bentley [b], L. Cecil Dharmasri [c]

[a] Department of Land Air and Water Resources, University of California, Davis, CA 95616, USA
[b] University of California Integrated Pest Management Program, Kearney Agriculture Center, Parlier, CA 93648, USA
[c] Syngenta Crop Protection, Inc., Greensboro, NC 27409, USA

ARTICLE INFO

Article history:
Received 13 August 2008
Accepted 6 March 2009

Keywords:
Aerial imagery
Integrated pest management
Partial Least Squares (PLS) regression
Prunus persica
Remote sensing
Spectral reflectance
Spectroradiometer

ABSTRACT

Remote sensing techniques can decrease pest monitoring costs in orchards. To evaluate the feasibility of detecting spider mite damage in orchards, we measured visible and near infrared reflectance of 1153 leaves and 392 canopies in 11 peach orchards in California. Pairs of significant wavelengths, identified by Partial Least Squares regression, were combined into normalized difference indices. These and 9 previously published indices were evaluated for correlation with mite damage.

Eight spectral regions for leaves and two regions for canopies (at blue and red wavelengths) were significantly correlated with mite damage. These findings were tested by calculating normalized difference indices from the Red and Blue bands of six multispectral aerial images.

Index values were linearly correlated with mite damage ($R^2 = 0.47$), allowing identification of mite hotspots in orchards. However, better standardization of aerial imagery and accounting for perturbing environmental factors will be necessary for making this technique applicable for early mite detection.

1. Introduction

Remotely sensed information is increasingly being used in modern agricultural production systems. While most efforts to detect crop statuses or processes affecting crops have focused on field crops (e.g., Idso et al., 1977; Wiegand et al., 1979; Tucker et al., 1981; Carley et al., 2008), several recent studies have looked into applications of remote sensing techniques in orchards. Perez-Priego et al. (2005) and Suarez et al. (2008) used spectral signatures of olive leaves and canopies for detecting water deficiency, while Sepulcre-Canto et al. (2007) related spectral information with olive yield and fruit parameters. In citrus, Ye et al. (2007) related the electromagnetic reflectance of canopies to yields, whereas Min and Lee (2005) used remotely sensed vegetation indices to approximate leaf nitrogen content. Other researchers have used remote sensing to estimate the chlorophyll content of orchard crops (Zarco-Tejada et al., 2004), the extent of chilling injury on citrus fruits (Menesatti et al., 2005) or infection of apple leaves with the fungus *Venturia inaequalis* (Cooke) Wint., the causal agent of apple scab (Delalieux et al., 2007).

In California, remote sensing is widely used in field crop production (Zhang et al., 2002, 2003, 2005; Fitzgerald et al., 2004; Qin and Zhang, 2005; Wang et al., 2008), but has so far found little to no application in tree crops. Due to the large extent of the fruit and nut production area in the state and the high value of the crops that are produced, improved monitoring and management strategies are needed to remain competitive in the increasingly global market for tree and nut crops. Such innovations are also necessary to meet presumably rising irrigation water costs and to manage agricultural pests in the face of tightened pesticide regulation.

Growers of peaches (*Prunus persica* L.) in California are currently facing particular economic strains. Historically, profit margins have been high for California peach growers, because of the state's favorable climate and strong domestic demand for fresh and canned peaches. In recent years, however, competition by foreign producers has increased substantially, with the value of imports from Chile already amounting to a quarter of the value of the national production (CDFA, 2008; FAO, 2008). This competition has led to a 9% decrease in the peach production area and a 27% drop in total production in California between 2004 and 2006 (CDFA, 2008).

Since farm wages cannot realistically be expected to decrease, technological progress seems the most viable way forward to increase the competitiveness of peach production in California. Remote Sensing can be a valuable tool for thoroughly monitoring orchards at low cost at a spatial resolution that is high enough to allow site-specific, economically favorable management strategies. Such strategies offer potential to reduce monitoring costs and enhance resource use efficiency, thus lowering total production

* Corresponding author.
E-mail address: mhzhang@ucdavis.edu (M. Zhang).

0303-2434/$ – see front matter © 2009 Elsevier B.V. All rights reserved.
doi:10.1016/j.jag.2009.03.002

costs and increasing the profit margins of farming operations. In peach production, such monitoring could be particularly useful in controlling and managing web-spinning spider mite damage early in the season.

While most other pests can be controlled quite effectively with one combined pesticide application early in the season, spider mite populations are often promoted by the early season pesticides, because these diminish the populations of mite predators, which then lag in numbers behind the proliferating mites. Consequently mite damage, caused mostly by the Pacific Spider Mite (*Tetranychus pacificus* McGregor) and the Two-spotted Mite (*Tetranychus urticae* Koch) in California peaches, typically occurs in the middle or towards the end of the growing season, requiring an extra spray, which according to the standard costs manual for peach production in California incurs additional costs of about 150 US$ ha^{-1} (Day et al., 2004).

In addition to being a cost factor, the typically applied and most effective miticides are classified as 'dangerous', and long Pre-Harvest Intervals (PHI) of up to 21 days have been imposed by the State of California (Fouche et al., 2000). For the most common miticide (active ingredient: propargite) used in California, the Restricted-Entry Interval (REI), during which the orchard can only be entered with protective clothing, is 21 days, more than ten times as long as for all other chemicals listed by Fouche et al. (2000). A miticide application can thus seriously disrupt the work flow in the orchard. Early detection of mite infestation would be highly desirable, since it would allow spraying against mites earlier in the season, allowing a better timing of late-season crop management and harvest. It would also facilitate more targeted control of mite hotspots in orchards or the more selective application of lower risk but more costly alternative miticides with shorter PHIs and REIs, thereby allowing growers to cut costs and reduce the orchard area that cannot be entered.

Mite hotspots often occur near the overwintering sites of adult females in protected places on trees or in litter, trash and weeds on the orchard floor. After becoming active in spring, mites begin feeding on weeds or lower parts of the peach trees (Pickel et al., 2006). They are favored by hot, dry conditions, and as temperatures rise during the spring and summer, they multiply and move up to the center of the tree, until the entire tree is infested. Dusty conditions in orchards often accelerate economically consequential mite damage, since mites are transported onto higher leaves with dust particles (Pickel et al., 2006). Consequently, mite infestations often occur first near dusty orchard roads.

Fitzgerald et al. (2004) showed that detection of mite damage in cotton (*Gossypium hirsutum* L.) caused by the strawberry spider mite (*Tetranychus turkestani* Ugar. & Nik.) using hyperspectral imagery is technically possible, and Peñuelas et al. (1995) detected damage caused by European Red Mites (*Panonychus ulmi* Koch) on apple trees.

The objective of this study was to test the feasibility of using remote sensing techniques for the detection of spider mite damage in peach orchards. To achieve this, we aim to identify suitable spectral wavelengths, the reflectance at which is correlated to mite damage on the leaf and on the canopy level. Furthermore, we will test, whether mite damage can be detected on multispectral aerial images. Finally, we will discuss the potential and limitations of applying remote sensing techniques to detect mite damage in California peach orchards.

2. Materials and methods

2.1. Study sites

This study was conducted in eleven peach orchards in Fresno and Kings Counties in California (Fig. 1). Three orchards were located at the University of California's Kearney Agriculture Center (KAC). All other orchards were privately managed by four growers. One of these growers operated two orchards (sites A and B in Fig. 1), and another grower's property was split into four subsections because of different varieties and planting densities in the orchard. These four orchards (site E in Fig. 1) were managed organically.

2.2. Sample collection and analysis

2.2.1. Leaf samples

A total of 1132 peach leaves were collected from nine orchards throughout the growing season of 2007. Leave samples were collected during calendar weeks 23, 25, 27, 30 and 32 (May 17th to July 19th). Because of the large number of study sites, not all orchards could be sampled at all points in time. To ensure comparability between the sampled leaves, all leaves were picked at a height of 2.5 m or less and from all regions of the canopy. Leaves that appeared abnormal, physically damaged or affected by pests other than mites were excluded from sampling. Only full-sized mature leaves were selected for further analysis. Care was also taken to select leaves from all areas of the orchards to make sure that all variation in environmental, microclimatic and soil conditions within the orchards was covered by leaf samples. All leaves were placed in sealed plastic bags and stored on ice until analysis.

Spectral data was collected under controlled conditions using an ASD FieldSpec Pro Field Spectroradiometer (Analytical Spectral Devices Inc., Boulder, CO, USA), which measures spectral reflectance between 350 and 2500 nm. The spectral resolution of this instrument is 3 nm at wavelengths between 350 and 1000 nm, and 10 nm for longer wavelengths, with spectral sampling intervals of 1.4 and 2 nm, respectively (ASD, 1999). Reflectance is expressed relative to the reflectance of a standardized white calibration surface. For measuring the leaf reflectance, a specially designed plant probe and leaf clip assembly device was attached to the instrument's fiber-optic cable to ensure standardized environmental conditions for reflectance measurement.

After calibrating the spectroradiometer according to the manufacturer's instructions, all leaf samples were reinspected for meeting the above requirements for comparability. For assessing the damage of each leaf, we then selected a region centering on the middle rib of the leaf. For this circular region with a diameter of 2.1 cm (area of 3.5 cm^2), we assessed the damage as an estimated percentage of the area that had sustained mite damage. Damage percentages were assigned in increments of 5 percentage points, except for very minor mite damage, which received a damage score of 1%. We preferred this damage assessment method over plant stress-based approaches, such as chlorophyll fluorescence (Bounfour et al., 2002), since methods based on damaged leaf surface area have been shown to more accurately describe the severity of mite damage (Skaloudova et al., 2006). A visual assessment was preferred over a computer-based approach (Skaloudova et al., 2006), since it allowed a larger number of samples to be analyzed and a clearer distinction between leaf damage caused by feeding spider mites vs. other plant stressors. Spider mites feeding on peach leaves cause a distinct mottling of the leaves, which can easily be distinguished from discolorations due to nutrient and water deficiency and most other pests and diseases (Pickel et al., 2006). Subsequently, the leaves were placed in the leaf clip device, and spectral reflectance patterns were determined as an average of three replicate measurements. To remove a jump in the spectral datasets at 975 nm, probably caused by spectral overlap between the three spectrometers included in the spectroradiometer (ASD, 1999), we used the jump correction algorithm in the software Spectral

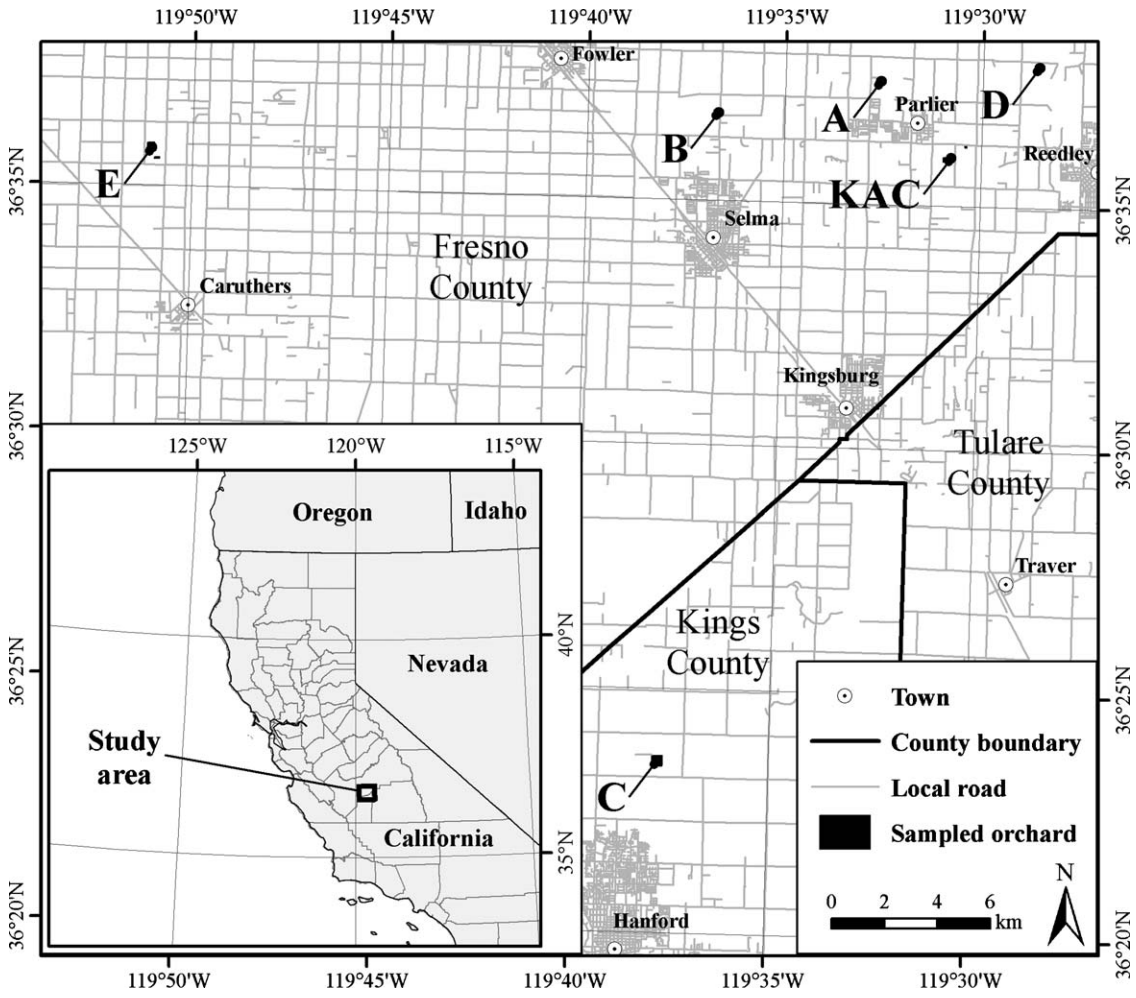

Fig. 1. Location of the sampled orchards in Fresno and Kings Counties, and location of the study area within the state of California (inset). Site KAC is the University of California's Kearney Agriculture Center, whereas sites A through E indicate the locations of private orchards. The three organically managed orchards are at site E.

Analysis and Measurement System (SAMS) Version 3.2 (University of California, Davis, CA, USA).

2.2.2. Canopy samples

In five orchards, a total of 392 tree canopies were sampled during calendar weeks 28, 30, 31, 32, 33, 35 (July 6th to August 22nd) of 2006. For examining the spectral reflectance of entire peach canopies, we used the spectroradiometer described above. Rather than using the leaf clip device to analyze leaves, however, we held the bare fiber-optic cable of the sensor vertically above the canopy of the trees at a distance of approximately 1 m. Given the spectroradiometer's field of view of 25°, each measurement thus summarized reflectance from a circular area of about 0.15 m^2. Reflectance signals were recorded in three replicates from two different locations in the canopy, resulting in a total of six measurements per tree. Since mite infestation levels in 2007 were so low that no mite damage gradient was available for study, data collection was restricted to the growing season of 2006.

As precisely estimating the percentage of a tree canopy that is affected by mite damage is difficult, mite damage ratings were assigned based on an estimate of damage severity, corresponding to the ratings suggested by Pickel et al. (2006), which are based on detailed inspections of the trees. Each tree was given a damage rating ranging from 0 (no damage) to 5 (severe damage). The criteria used to assign the damage ratings are listed in Table 1.

2.2.3. Mite counts

At weekly intervals between 13 June and 6 August 2006, 50 leaves were collected from each commercial orchard analyzed, and an additional 25 leaves from each block of the experimental orchard at KAC. All leaves were stored on ice until analysis. Spider mites and spider mite eggs were counted under the microscope.

2.2.4. Multispectral aerial images

For analyzing the feasibility of detecting mite damage using aerial imagery, we obtained six multispectral aerial images of one experimental orchard at Kearney Agriculture Center for the growing season of 2006 from a commercial image provider

Table 1
Criteria used to assign mite ratings at the canopy level during the visual inspection.

Damage class	Class name	Criteria
0	None	No visible mite damage
1	Low	An occasional mite on an occasional leaf
2	Low/moderate	Mites easier to find, but no colonies, no webbing, few eggs
3	Moderate	Some leaves without mites, other leaves with small colonies, eggs easy to find but very little webbing
4	Moderate/high	Mites on most leaves, colonies with eggs, webbing on some leaves
5	High	Lots of mites on most leaves, eggs and webbing abundant

(AgriData, Inc., Grand Forks, ND, USA). The images consisted of a Blue band (410–490 nm), a Green band (510–590 nm), a Red band (610–690 nm) and a Near Infrared band (800–900 nm). Images were taken at roughly weekly intervals between July 21st and August 21st, 2006.

2.3. Identification of significant wavelengths

Many processes that affect plant leaves are reflected in the spectral signature of the leaves. However, the degree, to which different wavelengths are correlated to such processes, varies widely, and identifying the most significant wavelengths within the spectrum requires advanced statistical tools. Because of the large number of variables contained in a spectral reflectance profile, which is often larger than the number of observed cases, and because of the often high collinearity between reflectances at different spectral wavelengths, ordinary regression methods tend to overfit prediction models. Several researchers have shown that Partial Least Squares regression (PLS; Wold, 1995; Wold et al., 1998) is a powerful tool to identify significant signals in such datasets (Frank and Friedman, 1993; Ourcival et al., 1999; Kooistra et al., 2003; Wilson et al., 2004; Min and Lee, 2005; Delalieux et al., 2007). The PLS algorithm iteratively produces a sequence of models, which use latent factors consisting of a linear combination of input variables, to explain the variation in the dependent variable. In order to determine the number of latent factors, most PLS implementations contain a cross-validation procedure, which uses a subset of the total number of cases to create a prediction model and tests this model against the remaining cases (Frank and Friedman, 1993). The cross-validation estimates the Prediction Residual Error Sum of Squares (PRESS) statistic for each number of latent factors, and selects the model, for which this indicator is minimized. Since a minimum is not always reached, and the maximum possible number of latent factors often overfits the prediction model, an end user decision about the number of latent factors is often necessary. Once the number of latent factors has been specified, the PLS procedure creates a coefficient matrix that can be interpreted as a descriptor of the relative significance of each wavelength of the spectrum (Min and Lee, 2005). We used the PLS algorithm implemented in JMP 7 (SAS Institute Inc., Cary, NC, USA) to correlate the leaf damage percentage to the spectral reflectance of the peach leaves.

For the canopy data, this regression was calculated based on the full reflectance spectrum and the damage class numbers. Even though the class numbers were assigned on an ordinal rather than a continuous scale, the PLS analysis should nevertheless allow an estimate of the most influential spectral regions for mite damage detection. As indicated by cross-validation, we chose four latent factors to explain the variability in the damage ratings. For the leaf analysis, the PRESS statistic of the cross-validation did not reach a minimum. To generate a dataset that is consistent over all scale levels analyzed in this study, we also assumed a model with four latent factors for the leaf data.

2.4. Construction of vegetation indices

For each region of significant wavelengths, we chose one representative band for the calculation of vegetation indices. For each of these regions, we selected the band representing the highest peak or deepest trough of the model parameter curve. To evaluate whether a region of PLS model parameters was significant, we followed the recommendation by Wold (1995), who suggested an absolute value threshold of 0.8. The selected bands for each significant region were then used to calculate vegetation indices from all possible permutations of two wavelengths among this set. In calculating indices, we followed the strategy of Hansen and Schjoerring (2003), who calculated normalized reflectance indices corresponding to the pattern of the Normalized Difference Vegetation Index (NDVI; Tucker, 1979) as RI $y - x = (r(\lambda_y) - r(\lambda_x))/(r(\lambda_y) + r(\lambda_x))$, in which $r(\lambda_x)$ and $r(\lambda_y)$ are the reflectances at wavelengths x and y, respectively. Whenever more than half of the calculated index values were negative, λ_x and λ_y were exchanged in the above equation to obtain positive values. This procedure was done separately for the leaf and canopy data.

The predictive capability of all such indices was tested by calculating linear regressions between each index and the damage percentage for all 1153 leaf samples and 392 canopy samples, respectively. Since most of these linear regressions yielded highly significant fits, goodness of fit was judged by interpreting the F value of the regression.

2.5. Comparison of results with existing vegetation indices

To examine the usefulness of the derived indices, the results were compared with the predictive capability of 9 previously published indices: the Normalized Difference Vegetation Index (NDVI; Rouse et al., 1974; Tucker, 1979), the Transformed Chlorophyll Absorption Ratio Index (TCARI; Haboudane et al., 2002), the Optimized Soil-Adjusted Vegetation Index (OSAVI; Haboudane et al., 2002), the Structure Insensitive Pigment Index (SIPI; Zarco-Tejada et al., 2005), the Corrected Transformed Vegetation Index (CTVI; Perry and Lautenschlager, 1984), the Modified Absorption in Reflectance Index (MCARI; Daughtry et al., 2000), the Soil-Adjusted Vegetation Index (SAVI; Huete, 1988), the Photochemical Reflectance Index (PRI; Gamon et al., 1992) and the Red Edge Vegetation Stress Index (RVSI; Perry and Davenport, 2007) (Table 2).

For all indices that required a definition of the red and near infrared part of the spectrum, we followed Tucker (1979), defining

Table 2
List of vegetation indices tested in this study.

Index name	Reference
Normalized Difference Vegetation Index: NDVI $= \frac{r_{NIR} - r_{Red}}{r_{NIR} + r_{Red}}$	Rouse et al. (1974); Tucker (1979)
Transformed Chlorophyll Absorption Ratio Index: TCARI $= 3 \cdot \left[(r_{700} - r_{670}) - 0.2 \cdot (r_{700} - r_{550}) \cdot \left(\frac{r_{700}}{r_{670}}\right)\right]$	Haboudane et al. (2002)
Optimized Soil-Adjusted Vegetation Index: OSAVI $= (1 + 0.16) \cdot \frac{(r_{800} - r_{670})}{r_{800} + r_{670} + 0.16}$	Haboudane et al. (2002)
Structure Insensitive Pigment Index: SIPI $= \frac{(r_{800} - r_{445})}{r_{800} - r_{680}}$	Zarco-Tejada et al. (2005)
Corrected Transformed Vegetation Index: CTVI $= \frac{(\mathrm{NDVI} + 0.5)}{\mathrm{abs}(\mathrm{NDVI} + 0.5)} \cdot \sqrt{\mathrm{abs}(\mathrm{NDVI} + 0.5)}$	Perry and Lautenschlager (1984)
Modified Absorption in Reflectance Index: MCARI $= [(r_{700} - r_{670}) - 0.2 \cdot (r_{700} - r_{550})] \cdot \left(\frac{r_{700}}{r_{670}}\right)$	Daughtry et al. (2000)
Soil-Adjusted Vegetation Index: SAVI $= \frac{r_{NIR} - r_{Red}}{r_{NIR} + r_{Red} + L} \cdot (1 + L)$, with $L = 1$	Huete (1988)
Photochemical Reflectance Index: PRI $= \frac{r_{570} - r_{531}}{r_{570} + r_{531}}$	Gamon et al. (1992)
Red Edge Vegetation Stress Index: RVSI $= \frac{r_{714} + r_{752}}{2} - r_{733}$	Perry and Davenport (2007)

red as radiation between 630 and 690 nm and near infrared as between 750 and 800 nm. As described above for the indices derived from the PLS regression, we calculated linear regressions between each of the previously published indices and the mite damage ratings and evaluated the goodness of the mite detection procedure by interpreting the *F* values.

2.6. Influence of site and season on index values

For quantifying the effects of site and season on index values, reflectance index values for leaves and canopies were analyzed using the Kruskal–Wallis test (Sokal and Rohlf, 1995), with orchard and calendar week as independent variables. To determine the impact of these effects on mite detection at the leaf level, we conducted separate analyses for healthy leaves and for damaged leaves that had more than 50% of the leaf area affected by mite damage. We restricted this analysis to the 10 indices that had the highest *F* values of the linear regression with mite damage. On the canopy level, we compared values of all 10 indices of healthy or mildly mite-affected canopies (damage classes 0 and 1) with index values of highly affected canopies (damage classes 4 and 5). To decide whether correction for site and date effects was necessary, we compared the distributions of index means of all orchard/date combinations for healthy and damaged leaves and canopies. If these distributions overlapped, reliable distinction of healthy leaves from one date or orchard from damaged leaves from another date or orchard was not possible in all cases, indicating a need for site- and date-specific correction. Since the scales of the various indices were widely different, we normalized all indices by subtracting the minimum index value and dividing by the range of index values for visualization and interpretation purposes. This transformation projected all indices onto a scale ranging from 0 to 1.

2.7. Transfer of canopy results to aerial images

To apply the results from the canopy analysis on the orchard level, we calculated reflectance indices from the Blue, Red and Near Infrared bands of the aerial images. The coarse spectral resolution of the aerial images unfortunately did not allow full application of the more detailed results obtained at the leaf and canopy levels. Red and Near Infrared were combined to calculate the NDVI, whereas the Red and Blue bands were used to calculate a NDVI-like Red–Blue index:

$$\text{Red}-\text{Blue index} = \frac{r_{Red} - r_{\text{Blue}}}{r_{\text{Red}} + r_{\text{Blue}}}$$

Unlike the NDVI, which reliably distinguishes vegetation in an image from non-vegetated areas, the Red–Blue index does not necessarily identify vegetation. To ensure that the analysis was restricted to the orchard trees, we calculated the NDVI, classified the images into two classes by using an equal-interval classification and interpreted the brighter of these classes as vegetated. All further analysis was then restricted to the vegetated area.

To remove some of the noise and provide more easily interpretable results, Red–Blue index images were then subjected to post-processing. To remove effects stemming from local variations in canopy density, we applied focal statistics on rectangular areas of 3×3 pixels, replacing each value by the maximum Red–Blue value encountered in the neighborhood of the pixel. The same function was then used to replace each pixel by the mean of a neighborhood area of 11×11 pixels. Since the resolution of the aerial images was 0.5 m, pixel values thus incorporated spectral information from a square area of 5.5 m $\times$ 5.5 m, being a good approximation of the size of a peach canopy.

The assignment of Red–Blue index values to the aerial images was investigated for images taken at Kearney Agriculture Center on July 21st and 29th and August 04th, 10th and 21st. Around the time of image capture, spider mite damage was assessed visually in the field by assigning damage classes, as described above for the canopy dataset. The size of the canopy of each tree was then digitized and the mean Red–Blue index calculated for the area of each sampled tree canopy. On average, each of the 75 trees used for verification was sampled 3.5 times during the season, resulting in a total of 265 pairs of damage ratings and index values for the verification dataset. To ensure that observable spatial difference in mite infestation levels occurred during the experiment, the orchard was split into eight blocks, four of which were sprayed with a broadband pesticide on June 14th, 2006 (see block delineations in Fig. 9). Since this application affects the natural predators of spider mites more strongly than the mites themselves, we expected more severe mite damage in the treated sections of the orchard.

Aerial imagery was only available as raw data, and radiometric calibration or atmospheric correction was impossible due to limited knowledge about the equipment used by the commercial provider and atmospheric conditions at the time of image capture. To still allow some comparison between images taken at different times during the season, we removed the linear bias of the calculated NDVI values by subtracting the minimum index value of each image from each pixel of the image. Linear regressions were then calculated between the corrected and uncorrected index values and the damage classes to test the accuracy of the

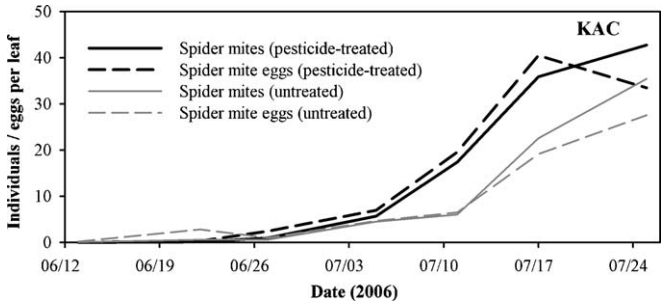

Fig. 2. Mean numbers of spider mites and spider mite eggs per leaf in pesticide-treated vs. untreated orchard blocks at Kearney Agriculture Center (KAC) over the 2006 sampling season.

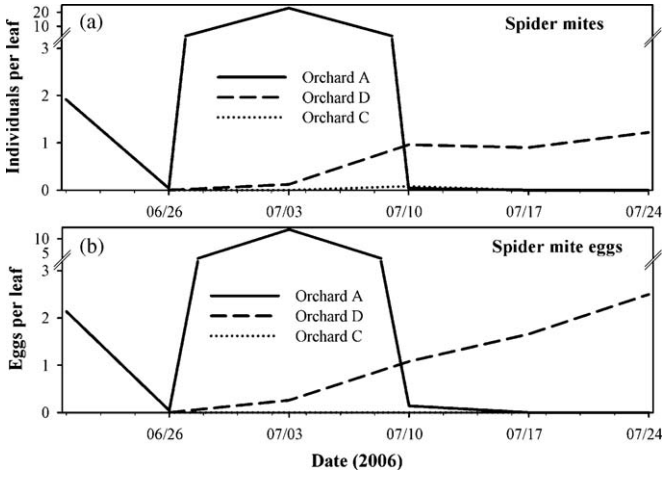

Fig. 3. Mean numbers of spider mites (a) and spider mite eggs (b) per leaf in three commercial peach orchards over the 2006 sampling season. Note the axis breaks in both plots, which were necessary to display the high early July concentrations in Orchard A.

classification. All spatial analyses were conducted using ArcGIS 9.2 (ESRI Inc., Redlands, CA, USA).

3. Results

3.1. Mite counts

Numbers of spider mites and spider mite eggs varied substantially between orchards and over time (Figs. 2 and 3). In the KAC orchards, application of broad-spectrum pesticides early in the season led to higher incidence of mites later (Fig. 2). Among the commercial orchards, orchard A temporarily had very high concentrations of web-spinning spider mites and eggs, but a miticide application in early July controlled mites effectively (Fig. 3). Orchard C had very low mite concentrations throughout the season. At Orchard D, mite and mite egg concentrations increased gradually, but did not reach levels at which the grower found it necessary to intervene.

3.2. Spectral signatures of peach leaves and canopies

While reflectance of healthy peach leaves was relatively low in the visible parts of the spectrum, with a peak in the green region, reflectance of near-infrared radiation was high, dropping off towards longer wavelengths (Fig. 4). Regions of low reflectance were found around the water absorption bands at 1450, 1900 and 2500 nm (Kou et al., 1993). The reflectance patterns of leaves that were heavily affected by mite damage were generally similar, but had higher reflectance in the visible region, lower reflectance in the nearest infrared, and higher reflectance around the water bands (Fig. 4).

For the tree canopies, reflectance was generally lower than for leaves at all except the water bands (Fig. 4), probably caused by the use of the bare fiber-optic cable of the sensor that did not have an artificial light source (ASD, 1999). Differences between healthy and mite-affected canopies persisted in the visible part of the spectrum. For near infrared radiation, the difference between

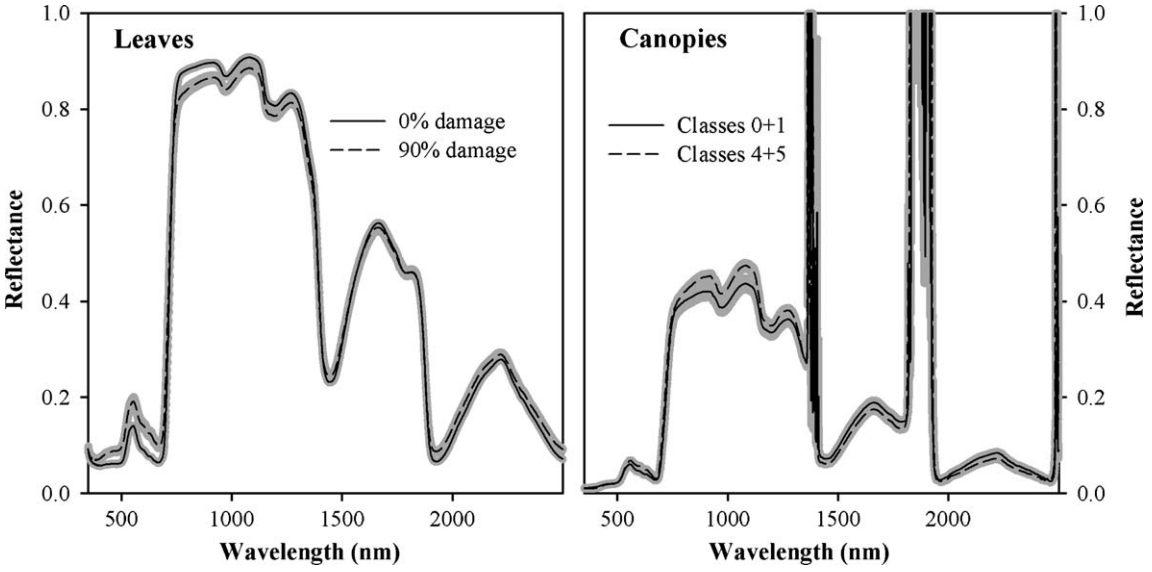

Fig. 4. Spectral reflectance profiles of all healthy and all heavily mite-affected peach leaves and canopies (0% and 90% of the leaf area damaged for the leaf dataset, and damage classes 0–1 and 4–5 for the canopies). The gray areas around the curves indicate ± one standard error of the mean.

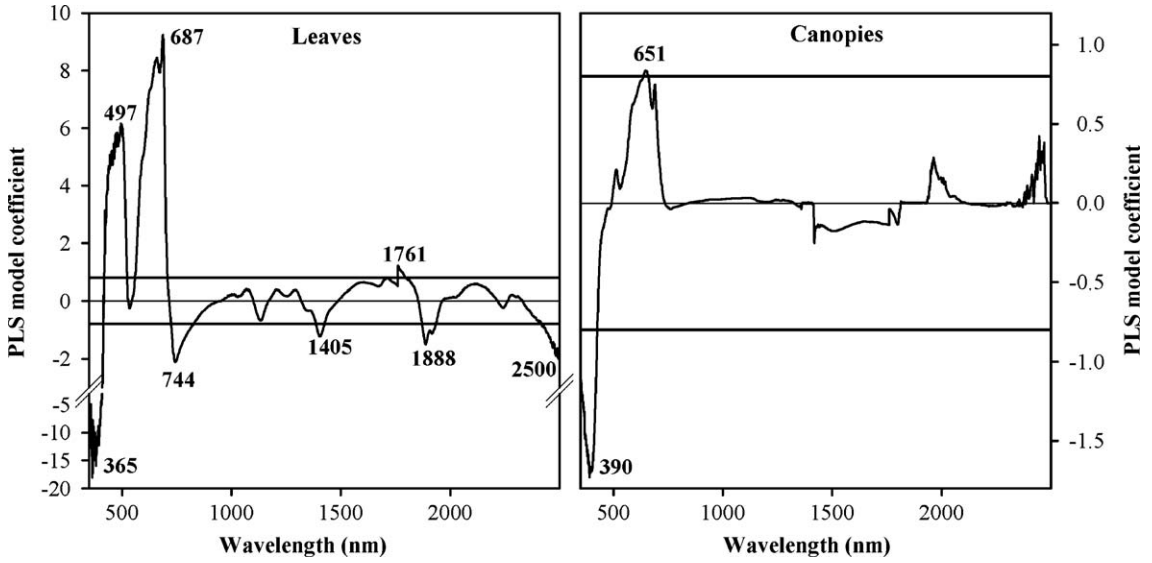

Fig. 5. Model coefficients of the Partial Least Squares (PLS) regression between reflectance at all spectral wavelengths analyzed and the numeric mite damage classification for data measured at the leaf (left graph) and canopy (right graph) level. The bold horizontal lines in both graphs indicate the thresholds at 0.8/−0.8, above/below which wavelengths were considered significant.

healthy and damaged leaves had the opposite sign of the differences detected on the leaf level, with healthy leaves ranging lower in reflectance than mite-affected leaves in the nearest infrared and higher at wavelengths between 1450 and 2500 nm (Fig. 4).

3.3. Significant wavelengths and reflectance indices for mite damage detection

The Partial Least Squares regression indicated that eight parts of the reflectance spectrum were significantly correlated with mite damage on the leaf level (Fig. 5). One significant region was in the blue and near ultraviolet part of the spectrum (with its highest absolute PLS model coefficient at 365 nm), one each occurred in the green (497 nm) and red (687 nm) regions, and another one was located at the top of the red edge (744 nm), in the nearest infrared. Three additional significant regions were located near the water absorption bands (1405, 1888 and 2500 nm). The abrupt peak at 1761 nm appears to be a measurement artifact, probably arising from spectral overlap between two of the three spectrometers contained in the spectroradiometer (ASD, 1999).

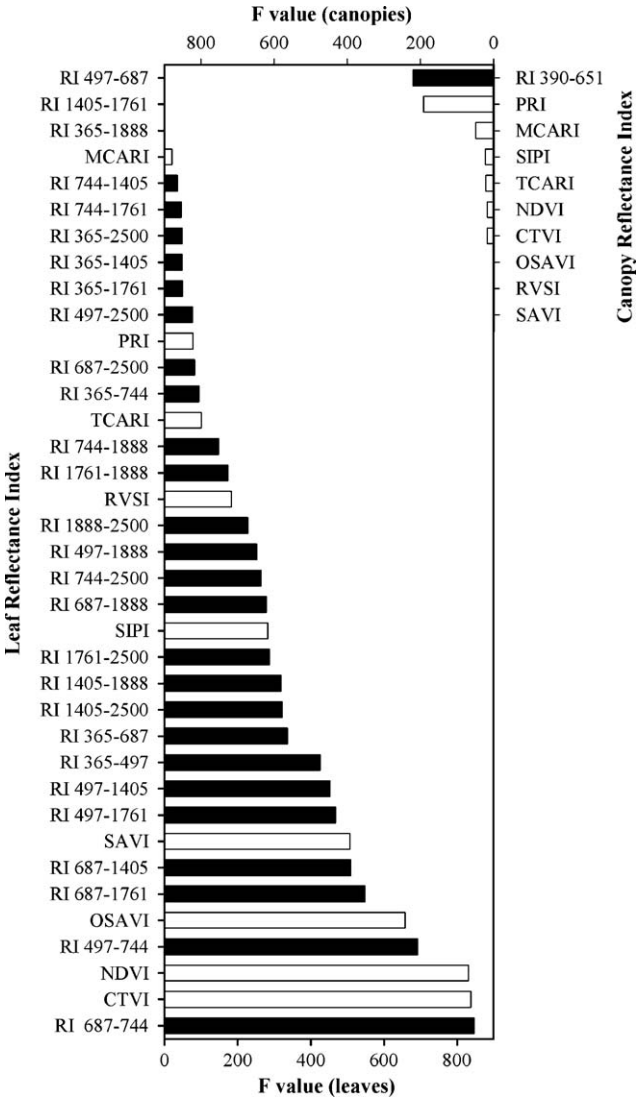

Fig. 6. *F* values of the linear regression between reflectance index values and mite damage rating for all indices investigated on the leaf (left and bottom axes) and canopy (right and top axes) level. White bars indicate previously published indices.

Only two significant regions were detected in the analysis of canopy level reflectance data (Fig. 5). These regions lay in the blue and near ultraviolet part of the spectrum (390 nm) and in the red region (651 nm).

Combining all possible pairs of two central bands of significant spectral regions into normalized difference reflectance indices resulted in a total of 28 indices for the leaf dataset and only one index for the canopy dataset. Adding the 9 previously published indices that were used to evaluate the usefulness of the newly derived indices (Table 2), this yielded a total of 37 indices on the leaf and 10 indices on the canopy level (Fig. 6). Values of the *F* statistic of linear regressions of these indices with mite damage varied widely, ranging from 0 to 847 for the leaf dataset and from 0 to 220 for the canopy dataset. On the leaf level, the most successful index was RI 687–744, followed by the CTVI, NDVI, RI 497–744 and OSAVI (Fig. 6). All of these indices exploit the difference between reflectances of red and near infrared radiation. On the canopy level, index RI 390–651 was most closely correlated with mite damage, followed by the PRI and, at a far lower *F* value, MCARI (Fig. 6). In contrast to the leaf level, all of these indices operate exclusively in the visible part of the spectrum. Indices that included infrared radiation did poorly on the canopy level, with *F* values of the linear correlation with mite damage ranging between 0 and 22, compared to 21, 49, 192 and 220 for the indices that solely relied on visible signals.

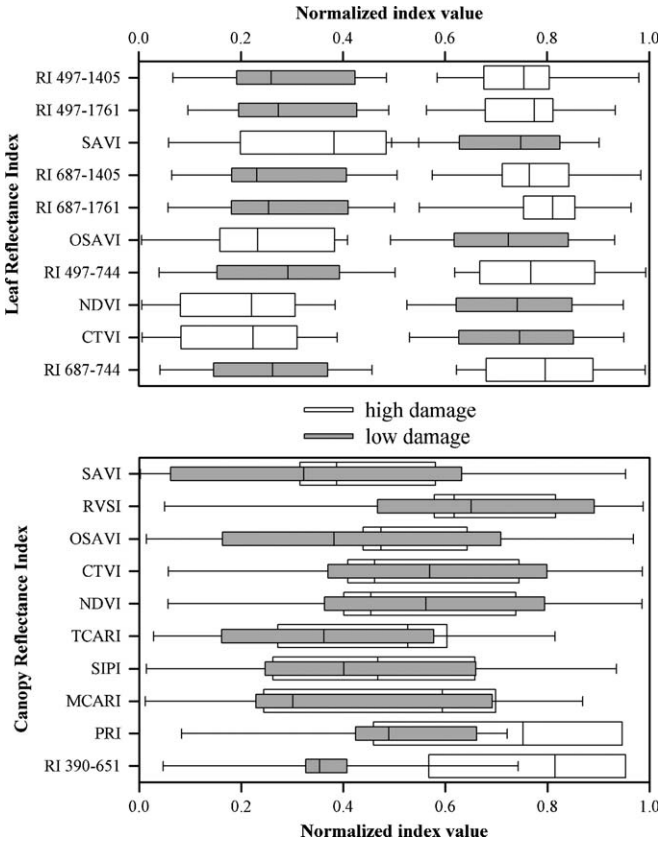

Fig. 7. Distributions of mean index values of all orchard/date combinations, for which leaf and canopy reflectance patterns were measured for healthy and heavily mite-affected peach leaves and canopies. All index values were linearly normalized to fit on a 0–1 scale, with 0 being the minimum and 1 the maximum index value. For leaves, mite-affected leaves had 50% or more of their area affected by mite damage, whereas healthy leaves showed no signs of damage. For canopies, damage ratings of 0 or 1 were considered healthy, whereas ratings above 3 were considered highly affected. In box plots, the center line is the median of the distribution, the edges of the boxes are the 25% and 75% quantiles, and the error bars indicate the 10% and 90% quantiles.

3.4. Influence of site and season on index values

Sampling site and sampling date effects were substantial on both the leaf and the canopy level for all indices. The Kruskal–Wallis test indicated that all effects of date and site on all indices were significant ($p < 0.05$). On the leaf level, however, the distributions of site/date-specific mean index values for healthy and damaged leaves showed no significant overlap for the ten most promising indices. This indicates that on the leaf level mite damage prediction based on these indices might be possible without correction for site or date effects (Fig. 7). On the canopy level, only one index (RI 390–651) showed potential for distinguishing between healthy and mite-affected trees without site- or date-specific correction, but achieved a less clear distinction than the analyses on the leaf level (Fig. 7).

3.5. Aerial images

Among the six aerial images analyzed, overall light intensity and shape of the value distribution histogram varied substantially for all color bands. Consequently, the value distribution of the NDVI and Red–Blue index, which were calculated from the Red, Blue and Near Infrared bands also showed a strong variation (Fig. 8). This variation was probably caused by the use of raw imagery. Removing the linear component of this bias by subtracting the minimum index value from each image projected the index values roughly onto the same scale between 0 and 0.16. After this adjustment, the index values were comparable and seemed useful for mapping spatial variation of mite damage within the orchard (Fig. 9). According to the visual impression created by a standard deviation based rendering of Adjusted Red–Blue index values, mite damage started on July 21st at the western, southern and eastern edge of the orchard and quickly spread to cover much of the eastern half of the field, including treatment block 7 (second from the south on the eastern side of the orchard in Fig. 9), which had not been sprayed with insecticide. In the western half of the orchard, the different mite damage levels created by the pesticide application were clearly visible. Until August 12th, the area affected by mite damage shifted slightly without strong changes in the general spatial pattern. For the image taken on August 16th, the distribution of the NDVI values differed from all other images, causing large parts of the image to be classified as non-vegetated. For this image, the image distortion caused by the use of raw image data was too large to be corrected by subtracting the minimum index value. Nevertheless, the mite damage distribution within the orchard did not seem overly affected, with the spatial pattern of the previous dates mostly preserved. By August 21st, areas affected by mite damage were mostly located in the southern part of the orchard, as well as on the western edge (Fig. 9).

Correlating the canopy mean of unadjusted Red–Blue index for the verification trees with the damage ratings assigned to these trees showed no significant correlation (Fig. 10), indicating that the spectral variation between images (Fig. 8) obscured any mite damage signals. After adjusting the index values of each image for the linear offset, however, the correlation improved, raising the coefficient of determination from 0.04 to 0.47. Since none of the verification trees was entirely unaffected by mites throughout the whole season, the verification only comprised damage classes 1 through 5. Even after adjusting the index values for the image-specific bias, substantial scatter remained in the dataset (Fig. 10).

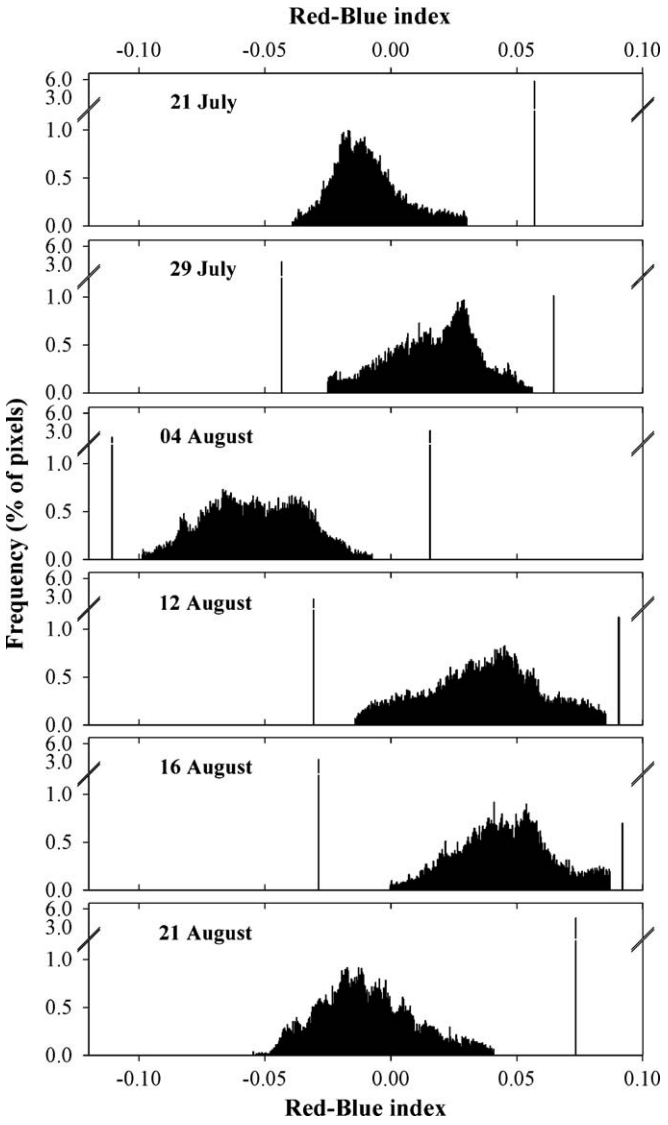

Fig. 8. Histograms of the Red–Blue index distribution among all pixels of aerial images of an experimental peach orchard at Kearney Agriculture Center taken on six different dates during the growing season of 2006.

4. Discussion

4.1. Spectral signature of mite damage

On the leaf level, mite damage was clearly reflected in the reflectance profiles, with significant differences appearing in various regions of the visible and near infrared regions of the electromagnetic spectrum. The model coefficients of the PLS regression indicated that the visible regions more strongly reflected mite damage than the longer wavelengths. When scaling up to the canopy level, however, all but two of these eight significant regions disappeared. Mite damage detection consequently seems easiest on the leaf level, indicating a higher potential for the development of ground-based spectral sensors than for aerial detection. Such ground-based sensors could be mounted on orchard equipment, such as fertilizer distributors or pesticide sprayers to provide spatially contiguous information on mite damage in orchards. This information could then be used to determine whether and where chemical treatment is necessary. When moving to the canopy scale, the spectral signal of mite damage was noticeably diluted by dust and water vapor in the air and by diffuse radiation from the surrounding area. In areas of dense vegetation, such as the peach orchards analyzed in this study, diffuse radiation should be particularly strong at near infrared wavelengths, simply because these wavelengths are almost completely reflected by vegetation. In analyses on the leaf level, diffuse radiation was kept to a minimum by shielding the

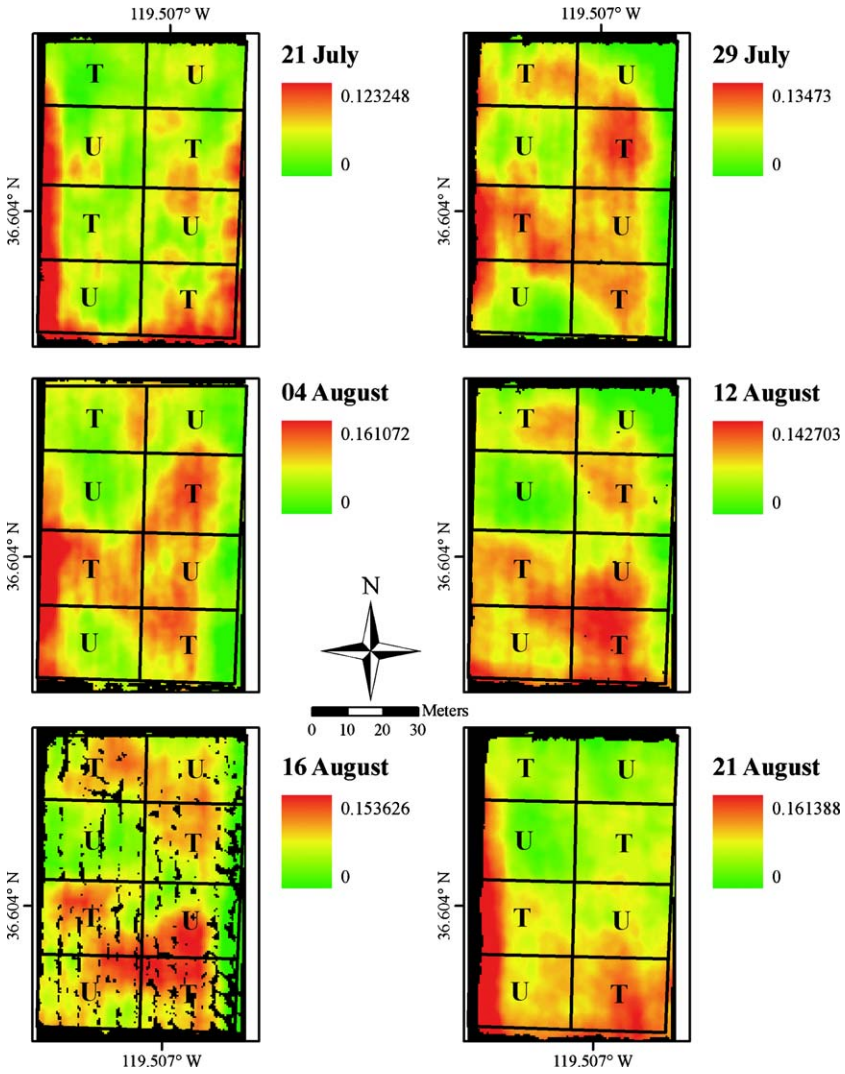

Fig. 9. Spatial distribution of Adjusted Red–Blue index values in the experimental peach orchard at Kearney Agriculture Center on six dates during the growing season of 2006. Index values are rendered using a standard deviation based algorithm. Note the different index maximum values for each date. The blocks in each image indicate sections of the orchard that were treated (T) or not treated (untreated – U) with broad-spectrum pesticides early in the season.

spectrometer's sensor from outside radiation, thus enabling the device to pick up the signals of decreased photosynthetic activity, water deficit and stress caused by mite damage (Reddall et al., 2004). Since the near infrared wavelengths that are mainly affected by these processes are not useful for analyses on the canopy level, the only effect of mite damage that can reliably be picked up at this level appears to be a change in leaf color. The shift from dark green to yellowish or even reddish tones that is typically caused by spider mites is reflected in the visible part of the spectrum, the reflectance readings of which are much less affected by diffuse radiation than those at longer wavelengths. This indicates potential of using sensors based on greenness indices, which are already commercially available.

4.2. Usefulness of reflectance indices for detecting mite damage

At the leaf level, the majority of reflectance indices analyzed was significantly correlated with mite damage and even promising to some degree for developing a mite detection algorithm. The reason for this is probably that mite damage affects peach leaves on a very fundamental level, with implications for the leaves' water balance, photosynthetic activity, chlorophyll content and level of physiological stress (Reddall et al., 2004). All of these states and processes have characteristic signatures, which can be detected by spectral analysis. All indices based on the difference between visible reflectance and reflectance at the water absorbing bands, such as RI 687–1405, RI 365–1888 or RI 497–2500, mirror the water deficit of the leaves, indices based on differences between red and near infrared radiation indicate photosynthetic capacity (Sellers, 1985; CTVI, NDVI, OSAVI), and indices at the red edge reflect plant stress (RI 687–744). All of these indices require near infrared reflectance, which is often used for detecting vegetation but appears less useful for identifying subtle differences in the reflectance of larger areas of intense vegetation. The diffuse radiation at these wavelengths appears to cover up most signals created by plant physiological processes. Consequently, both indices that showed potential for detecting mite damage on the canopy scale (RI 390–651 and PRI) were in the visible parts of the spectrum, reflecting discolorations that can be detected with the naked eye. Both indices reflect the color shift from the blue and green appearance of healthy leaves to the reddish yellow tones caused by mite damage. These results correspond to the findings of Peñuelas et al. (1995), who found the highest potential for detecting damage by European Red Mites for indices operating at visible wavelengths.

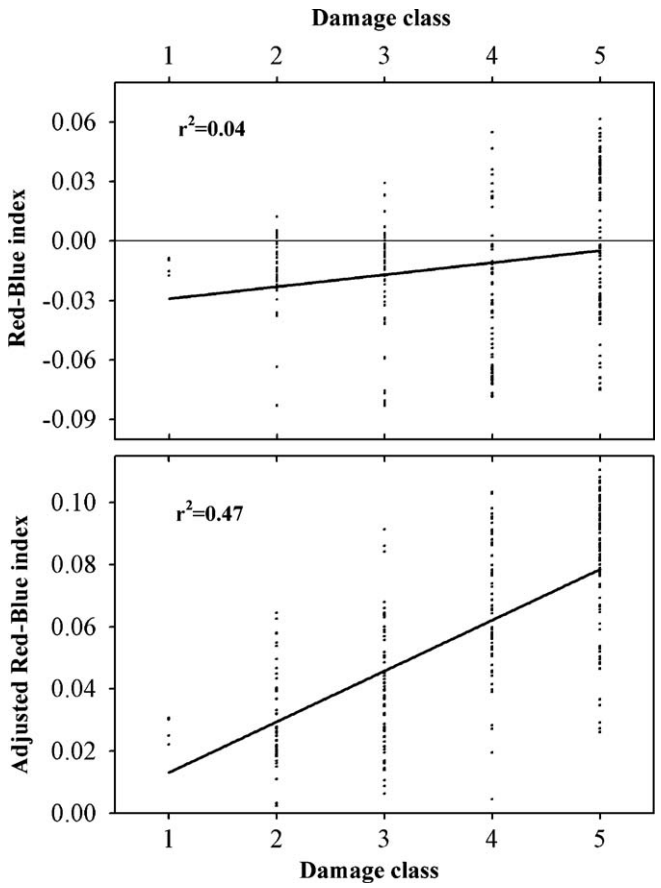

Fig. 10. Correlation of mite damage ratings of sample trees with unadjusted and adjusted Red–Blue index values. Damage ratings were based on visual appraisal of tree state, and all index values were averaged over the area covered by the tree canopy.

4.3. Aerial images

Since aerial images are not commonly available at the high spectral resolution of the field spectrometer, the range of wavelengths that can be exploited for mite damage detection is further decreased by moving to the aerial level. Fortunately, the canopy analyses indicated that mite damage affects fairly large regions in the red and blue parts of the electromagnetic spectrum (Fig. 5), which are covered by the aerial images. A Red–Blue index thus appeared promising for detecting mite damage in the sample orchard. When scaling up to the aerial image level, however, several confounding factors were introduced in addition to the loss of spectral resolution. Water vapor, dust and diffuse radiation, while already a problem at the canopy scale, can become serious impediments to accurate analysis of electromagnetic spectra based on aerial images. In addition to that, images taken from the air normally cover large areas, with often considerable distortion of some or all wavebands at increasing distances from the plane's nadir. The extent, to which such effects impact spectral analysis, depends on the kind of equipment used and the amount and quality of post-processing done on the images. For images that are obtained from commercial providers, these factors are often unknown or beyond the orchard manager's control. The success of any remote sensing applications in fruit orchards will depend on how well these factors can be accounted for or eliminated. The absence of remote sensing use from orchards, in spite of a growing body of literature indicating potential for use in fruit production, indicates that more efforts need to be undertaken to standardize aerial imagery and to eliminate some of the distorting factors. In our analysis, the biggest constraint to image usefulness was the considerable variation in the spectral patterns throughout the season caused by the use of raw imagery (Fig. 8). While we were able to correct for some of this variation by removing the linear bias, the uncertainty about the effects of this correction on the maximum index values made us stop short of defining a scale for absolute mite damage levels. The rise and fall of maximum index values throughout the season (Fig. 9) was at odds with our observation of a gradual rise in mite infestation, indicating the need for further adjustment of the spectral reflectance profiles. The development of an absolute mite damage scale would therefore require a much larger set of orchards, more extensive ground observations of damage levels, and a more thorough approach to spectral correction. We assume that these difficulties stem from the relative complexity of orchard ecosystems compared to annual field crops, in which remote sensing has been very successful. While in annual crops most of the variation between the spectral profiles of healthy plants at different sites can be explained by differences in soil type, season and a limited range of possible management options, the reflectance of orchard trees is likely influenced by a host of additional factors, such as Leaf Area Index, age of the trees, planting density, pruning regime, variety or intensity and type of understory vegetation.

Nevertheless, detecting relative mite damage levels within an orchard was clearly possible. The elevated levels of mite incidence that were caused by insecticide application to some of the blocks in the field was visible on the aerial images, even though the effect of the treatment was smaller than expected, probably because of the relatively small size of the experimental blocks. More importantly, the progression of mite damage was visible in the image time series. As would be expected based on the University of California's pest management guidelines (Pickel et al., 2006), mite damage first occurred near the edges of the orchard, where dusty conditions, promoted by an adjacent dirt road, probably facilitated initial mite dispersal. In spreading towards the orchard's interior, it remained relatively low in the blocks where no pesticides had been sprayed, indicating that mites in these areas were controlled relatively effectively by their natural enemies (Pickel et al., 2006). Overall the correspondence of Adjusted Red–Blue index values with the levels of mite damage observed on the sampled trees (Fig. 10) confirmed the usefulness of this index.

4.4. Feasibility of using remote sensing for mite damage detection

Our study clearly showed that mite damage on peach leaves evokes a spectral response that can be observed on the leaf as well as on the canopy level. While more work needs to be done on transferring these findings to the scale of aerial images, our analysis also indicated that using remote sensing for mite damage detection could be technically feasible on that level. The potential of remote sensing in orchards seemed greater at visible wavelengths than in the near infrared. This contradicted the findings of Delalieux et al. (2007), who concluded that near infrared radiation had greater potential for detecting apple scab based on a study that focused only on the leaf level. Nevertheless, in the absence of a reliable scale and with the variability inherent in many commercially available aerial images, early detection of mite outbreaks seems difficult. Another constraint to aerial detection of mite outbreaks is the typical spreading pattern of mites on individual peach trees. In most cases, mites start colonizing a tree from the bottom, initially affecting the part of the canopy that is least likely to be visible on aerial images. By the time mite damage has become severe enough to result in a clear spectral signal that is detectable by a camera mounted on an airplane, trees are likely to already be severely affected. More calibration and verification efforts have to be invested in this technology, before a final decision about its potential for early mite detection can be made. In particular, the

effects of other factors and processes that affect leaf color, such as water or nutrient deficiencies, needs to be elucidated.

Currently, the Red–Blue index is useful for detecting patterns in mite damage, which can be used for identifying hotspots of mite damage and for targeting pest control measures. It remains doubtful, whether this application alone can make the use of remote sensing economically feasible for California peach growers. We are confident that this technology holds potential for the high-value stonefruit industry of California, if early detection of mites and/or other important orchard pests becomes possible, or if pest monitoring applications can be coupled with other uses of remote sensing. The high correlation of leaf level readings with mite damage makes it likely that ground-based sensors will achieve better damage detection results than aerial sensors.

5. Conclusions

Mite damage on peaches clearly elicits a response in the spectral reflectance patterns of both leaves and entire canopies. While the leaf analysis showed that many wavelengths of the near infrared spectrum carry information on mite damage, these signals were not significant on the canopy scale, due to absorption by dust and water vapor and signal dilution by diffuse radiation. Only the signal caused by discoloration was preserved on the canopy scale, and could also be picked up in the analysis of aerial photographs, allowing spatially explicit mapping of relative mite damage in the orchard. Before this methodology can be transferred into practical orchard management, an absolute scale must be determined, on which mite damage can reliably be estimated. If such a scale can be found, remote sensing could become a useful tool for early detection of mite outbreaks in peach orchards. For making use of the high correlation of leaf-level indices with mite damage, the suitability of ground-based sensors for early detection of spider mite damage should be evaluated.

Acknowledgments

We are grateful for the friendly cooperation of the California peach growers Bill Chandler, Mark Nakata, Ty Parkinson and Peter Tos, as well as the field staff at Kearney Agriculture Center. Generous funding by the United States Environmental Protection Agency under the Food Quality Protection Act and by the California Department of Pesticide Regulation is highly appreciated.

References

ASD, 1999. Analytical Spectral Devices Technical Guide, fourth edition. Analytical Spectral Devices, Inc., Boulder, CO, USA.

Bounfour, M., Tanigoshi, L.K., Chen, C., Cameron, S.J., Klauer, S., 2002. Chlorophyll content and chlorophyll fluorescence in red raspberry leaves infested with Tetranychus urticae and Eotetranychus carpini borealis (Acari: Tetranychidae). Environ. Entomol. 31, 215–220.

Carley, D.S., Jordan, D.L., Dharmasri, L.C., Sutton, T.B., Brandenburg, R.L., Burton, M.G., 2008. Peanut response to planting date and potential of canopy reflectance as an indicator of pod maturation. Agron. J. 100, 376–380.

CDFA, 2008. California Agricultural Resource Directory 2007. California Department of Food and Agriculture, Sacramento, CA, USA.

Daughtry, C.S.T., Walthall, C.L., Kim, M.S., de Colstoun, E.B., McMurtrey, J.E., 2000. Estimating corn leaf chlorophyll concentration from leaf and canopy reflectance. Remote Sens. Environ. 74, 229–239.

Day, K.R., Andris, H.L., Klonsky, K.M., De Moura, R.L., 2004. Sample Costs to Establish and Produce Peaches—Fresh Market. University of California Cooperative Extension, Davis, CA, USA.

Delalieux, S., van Aardt, J., Keulemans, W., Schrevens, E., Coppin, P., 2007. Detection of biotic stress (*Venturia inaequalis*) in apple trees using hyperspectral data: non-parametric statistical approaches and physiological implications. Eur. J. Agron. 27, 130–143.

FAO, 2008. FAOSTAT Database. Food and Agriculture Organization of the United Nations, Rome, Italy.

Fitzgerald, G.J., Maas, S.J., Detar, W.R., 2004. Spider mite detection and canopy component mapping in cotton using hyperspectral imagery and spectral mixture analysis. Precis. Agric. 5, 275–289.

Fouche, C., Molinar, R., Canevari, M., Joshel, C., Mullen, B., Weber, J., 2000. Pesticides for Specialty Crops. Division of Agriculture and Natural Resources, University of California, Oakland, CA, USA.

Frank, I.E., Friedman, J.H., 1993. A statistical view of some chemometrics regression tools. Technometrics 35, 109–135.

Gamon, J.A., Peñuelas, J., Field, C.B., 1992. A narrow-waveband spectral index that tracks diurnal changes in photosynthetic efficiency. Remote Sens. Environ. 41, 35–44.

Haboudane, D., Miller, J.R., Tremblay, N., Zarco-Tejada, P.J., Dextraze, L., 2002. Integrated narrow-band vegetation indices for prediction of crop chlorophyll content for application to precision agriculture. Remote Sens. Environ. 81, 416–426.

Hansen, P.M., Schjoerring, J.K., 2003. Reflectance measurement of canopy biomass and nitrogen status in wheat crops using normalized difference vegetation indices and partial least squares regression. Remote Sens. Environ. 86, 542–553.

Huete, A.R., 1988. A soil-adjusted vegetation index (SAVI). Remote Sens. Environ. 25, 295–309.

Idso, S.B., Jackson, R.D., Reginato, R.J., 1977. Remote-sensing of crop yields. Science 196, 19–25.

Kooistra, L., Leuven, R., Wehrens, R., Nienhuis, P.H., Buydens, L.M.C., 2003. A comparison of methods to relate grass reflectance to soil metal contamination. Int. J. Remote Sens. 24, 4995–5010.

Kou, L.H., Labrie, D., Chylek, P., 1993. Refractive-indices of water and ice in the 0 65- to 2.5-μm spectral range. Appl. Opt. 32, 3531–3540.

Menesatti, P., Urbani, G., Lanza, G., 2005. Spectral imaging VIS-NIR to forecast the chilling injury onset on citrus fruits. Acta Hort. 682, 1347–1354.

Min, M., Lee, W.S., 2005. Determination of significant wavelengths and prediction of nitrogen content for citrus. T. ASAE 48, 455–461.

Ourcival, J.M., Joffre, R., Rambal, S., 1999. Exploring the relationships between reflectance and anatomical and biochemical properties in *Quercus ilex* leaves. New Phytol. 143, 351–364.

Peñuelas, J., Baret, F., Filella, I., 1995. Semiempirical indexes to assess carotenoids/chlorophyll-a ratio from leaf spectral reflectance. Photosynthetica 31, 221–230.

Perez-Priego, O., Zarco-Tejada, P.J., Miller, J.R., Sepulcre-Canto, G., Fereres, E., 2005. Detection of water stress in orchard trees with a high-resolution spectrometer through chlorophyll fluorescence in-filling of the O-2-A band. IEEE Trans. Geosci. Remote Sens. 43, 2860–2869.

Perry, C.R., Lautenschlager, L.F., 1984. Functional equivalence of spectral vegetation indices. Remote Sens. Environ. 14, 169–182.

Perry, E.M., Davenport, J.R., 2007. Spectral and spatial differences in response of vegetation indices to nitrogen treatments on apple. Comput. Electron. Agric. 59, 56–65.

Pickel, C., Bentley, W.J., Hasey, J.K., Day, K.R., Gubler, W.D., Adaskaveg, J.E., Westerdahl, B.B., McKenry, M.V., Shreshta, A., Lanini, W.T., Hembree, K.J., 2006. UC IPM Pest Management Guidelines: Peach. UC Statewide Integrated Pest Management Program, University of California, Oakland, CA, USA.

Qin, Z., Zhang, M., 2005. Detection of rice sheath blight for in-season disease management using multispectral remote sensing. Int. J. Appl. Earth Obs. Geoinf. 7, 115–128.

Reddall, A., Sadras, V.O., Wilson, L.J., Gregg, P.C., 2004. Physiological responses of cotton to two-spotted spider mite damage. Crop Sci. 44, 835–846.

Rouse, J.W., Haas, R.H., Schell, J.A., Deering, D.W., Harlan, J.C., 1974. Monitoring the vernal advancements and retrogradation of natural vegetation. NASA/GSFC, Greenbelt, MD, USA.

Sellers, P.J., 1985. Canopy reflectance, photosynthesis and transpiration. Int. J. Remote Sens. 6, 1335–1372.

Sepulcre-Canto, G., Zarco-Tejada, P.J., Jimenez-Munoz, J.C., Sobrino, J.A., Soriano, M.A., Fereres, E., Vega, V., Pastor, M., 2007. Monitoring yield and fruit quality parameters in open-canopy tree crops under water stress Implications for ASTER. Remote Sens. Environ. 107, 455–470.

Skaloudova, B., Krivan, V., Zemek, R., 2006. Computer-assisted estimation of leaf damage caused by spider mites. Comput. Electron. Agric. 53, 81–91.

Sokal, R.R., Rohlf, F.J., 1995. Nonparametric methods in lieu of single classification ANOVAs. In: Sokal, R.R. (Ed.), Biometry: The Principles and Practice of Statistics in Biological Research. W.H. Freeman, New York, NY, USA, pp. 423–439.

Suarez, L., Zarco-Tejada, P.J., Sepulcre-Canto, G., Perez-Priego, O., Miller, J.R., Jimenez-Munoz, J.C., Sobrino, J., 2008. Assessing canopy PRI for water stress detection with diurnal airborne imagery. Remote Sens. Environ. 112, 560–575.

Tucker, C.J., 1979. Red and photographic infrared linear combinations for monitoring vegetation. Remote Sens. Environ. 8, 127–150.

Tucker, C.J., Holben, B.N., Elgin, J.H., McMurtrey, J.E., 1981. Remote-sensing of total dry-matter accumulation in winter-wheat. Remote Sens. Environ. 11, 171–189.

Wang, X., Zhang, M., Zhu, J., Geng, S., 2008. Spectral prediction of *Phytophthora infestans* infection on tomatoes using artificial neural network (ANN). Int. J. Remote Sens. 29, 1693–1706.

Wiegand, C.L., Richardson, A.J., Kanemasu, E.T., 1979. Leaf area index estimates for wheat from Landsat and their implications for evapotranspiration and modeling. Agron. J. 71, 336–342.

Wilson, M.D., Ustin, S.L., Rocke, D.M., 2004. Classification of contamination in salt marsh plants using hyperspectral reflectance. IEEE Trans. Geosci. Remote Sens. 42, 1088–1095.

Wold, S., 1995. PLS for multivariate linear modeling. In: van der Waterbeemd, H. (Ed.), Chemometric Methods in Molecular Design: Methods and Principles in Medicinal Chemistry. Verlag-Chemie, Weinheim, Germany, pp. 195–218.

Wold, S., Antti, H., Lindgren, F., Ohman, J., 1998. Orthogonal signal correction of near-infrared spectra. Chemometr. Intell. Lab. 44, 175–185.

Ye, X.J., Sakai, K., Manago, M., Asada, S., Sasao, A., 2007. Prediction of citrus yield from airborne hyperspectral imagery. Precis. Agric. 8, 111–125.
Zarco-Tejada, P.J., Miller, J.R., Morales, A., Berjon, A., Aguera, J., 2004. Hyperspectral indices and model simulation for chlorophyll estimation in open-canopy tree crops. Remote Sens. Environ. 90, 463–476.
Zarco-Tejada, P.J., Ustin, S.L., Whiting, M.L., 2005. Temporal and spatial relationships between within-field yield variability in cotton and high-spatial hyperspectral remote sensing imagery. Agron. J. 97, 641–653.
Zhang, M., Liu, X., O'Neill, M., 2002. Spectral discrimination of *Phytophthora infestans* infection on tomatoes based on principal component and cluster analyses. Int. J. Remote Sens. 23, 1095–1107.
Zhang, M., Qin, Z., Liu, X., 2005. Remote sensed spectral imagery to detect late blight in field tomatoes. Precis. Agric. 6, 489–508.
Zhang, M., Qin, Z., Liu, X., Ustin, S.L., 2003. Detection of stress in tomatoes induced by late blight disease in California, USA, using hyperspectral remote sensing. Int. J. Appl. Earth Obs. Geoinf. 4, 295–310.